

Hurst Parameter Estimation of Long-Range Dependent VBR MPEG Video Traffic in ATM Networks¹

Seung Hoon Hong, Rae-Hong Park, and Chang Bum Lee

Department of Electronic Engineering, Sogang University, C.P.O. Box 1142, Seoul 100-611, Korea

Received April 26, 1999; accepted August 9, 2000

Video is becoming the most important data in asynchronous transfer mode (ATM) networks. In ATM networks, image quality remains almost the same by encoding a video signal at variable bit rates (VBRs). Moving picture experts group (MPEG) video consists of three different frames: intra (I), predictive (P), and bidirectional (B). The important feature of VBR MPEG video traffic is the long-range dependence (LRD) characteristic. To examine the LRD characteristic of real MPEG video sequences, the Hurst parameter is employed. This paper presents a wavelet method, a line length method, and a Fourier filtering method for Hurst parameter estimation and compares their performance of LRD analysis with various video data. The relationship between the Hurst parameter and parameters in fractal modeling is also investigated. © 2001 Academic Press

1. INTRODUCTION

To overcome the bandwidth limitation of the conventional narrowband-integrated services digital network (N-ISDN) and to effectively deal with the services requiring various transmission characteristics, broadband-ISDN (B-ISDN) has been developed. To implement B-ISDN, asynchronous transfer mode (ATM) with the network structure independent of the transmission speed and characteristics of information sources was proposed. The most important communication services in B-ISDN are video services that require wide bandwidth. Video services in B-ISDN include videophone, videoconference, high definition television (HDTV), and TV broadcasting. B-ISDN can process various types of services together, as the base of a communication network, and offers economic and convenient multimedia services such as voice, data, and video applications.

In ATM networks, image quality remains almost the same by encoding a video signal at variable bit rates (VBRs). To realize video communication in ATM networks, we must consider the transmission flexibility and constraint of ATM networks. Efficient video coding methods [1] and network resource applications are also required. Video signals with a large

¹ This work was supported in part by the Electronics and Telecommunication Research Institute, Taejeon, Korea.

amount of data are required for real-time processing and their bit rates show the bursty characteristic [2]. Statistical characteristics of the standard video traffic such as moving picture experts group (MPEG) have been investigated. The traffic control and bandwidth allocation techniques of conventional communication networks are likely to be congested. To satisfy different qualities of service (QoS) for the calls with various transmission characteristics, efficient traffic control mechanisms are required over processes of transmission.

It is important to reliably model the traffic source for effective traffic control in ATM networks [3]. Conventional methods of modeling voice and data are simple, whereas a more sophisticated method is required for modeling video traffic. By measuring characteristics of VBR video traffic, traffic has recently been effectively represented by statistical self-similarity, which is explained by the long-range dependence (LRD) characteristic. If self-similarity is employed, both the short-term and long-term bursty characteristics are easily explained. The LRD characteristic of VBR video traffic can be measured by the Hurst parameter. This paper presents three Hurst parameter estimation methods, compares their performance of LRD analysis, and describes applications to fractal modeling of video traffic.

2. CHARACTERISTICS OF VBR MPEG VIDEO TRAFFIC

An MPEG encoder generates three types of frames, namely, the intra (I) frame, the predictive (P) frame, and the bidirectional (B) frame [4, 5]. The group of these frames is called the group of picture (GOP). Figure 1 shows the structure of the GOP. The I frame is the access point of a GOP and is encoded by the discrete cosine transform (DCT) and quantization. It does not use any information in the past and future frames; thus, it reduces accumulated error. The bit rate of the I frame is larger than those of the P and B frames; however, the number of I frames in a GOP is smaller than the number of P and B frames. The P frame contains information obtained by predicting with the latest I or P frames, in which temporal redundancy is reduced by motion compensation. The B frame is generated by predicting bidirectionally with I and P frames or with two P frames immediately adjacent to it. The B frame yields a compression ratio larger than those of the P and I frames, with smaller variations of the bit rate.

The VBR MPEG video sequences used in experiments consist of movies, sports, shows, and others [6]. Each video sequence consists of 40,000 frames, equivalent to approximately a 30-min sequence except for the Video Conference sequence (3 min) and the News Show

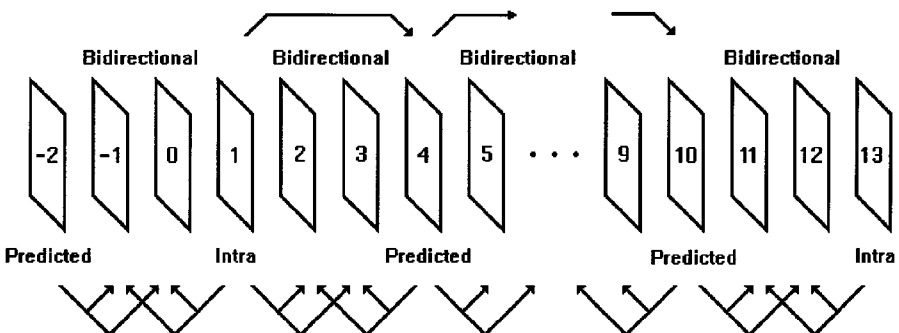


FIG. 1. Structure of GOP.

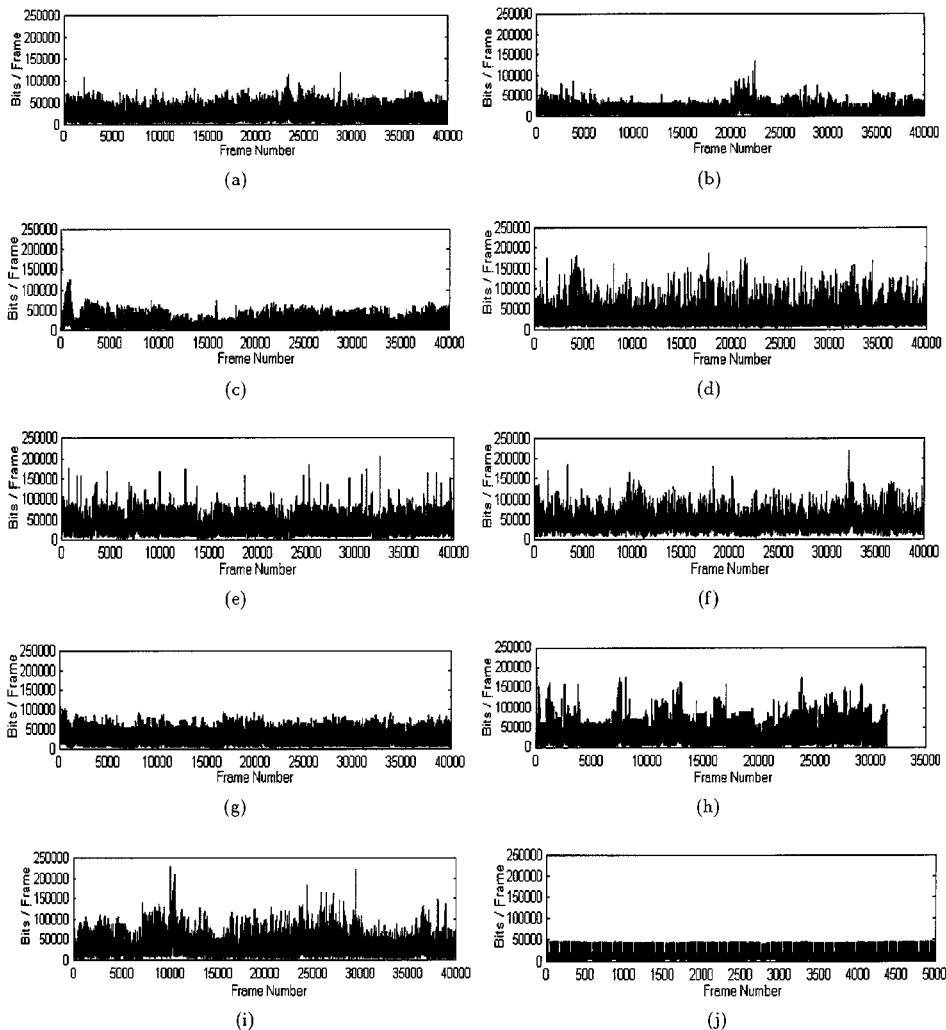


FIG. 2. Bit rate fluctuations of various VBR MPEG video sequences used in experiments: (a) Jurassic Park; (b) The Silence of the Lambs; (c) Star Wars; (d) Soccer World Cup Final 1994, Brazil-Italy; (e) ATP Tennis Final 1994, Becker-Sampras; (f) Formula 1 Race, GP Hockenheim 1994; (g) Talk Show; (h) TV News Show; (i) MTV Music Video Clips; (j) Video Conference.

sequence (18 min). Figure 2 shows bit rate fluctuations of various VBR MPEG video sequences used in experiments. The compression rate R , the mean m , and the standard deviation σ of the bit rate, and burstiness B defined by the ratio of the peak bit rate to the mean bit rate, are shown in Table I for each sequence, where the statistical quantities are listed for three cases: quantities in frame unit, quantities in GOP unit, and quantities per second. Table II shows the parameters of the MPEG-I encoder for the bit stream used in experiments.

3. HURST PARAMETER ESTIMATION

3.1. Long-Range Dependence

In video traffic with the LRD characteristic, the decreasing rate of the autocorrelation function is much slower than that of the exponential function. Let $X(t) = (X_t; t =$

TABLE I
Statistical Characteristics of Each Video Sequence

Sequence	Frames				GOPs			Bit rate		
	R	m [Kbits]	$\sigma [\times 10^3]$	B	m [Kbits]	$\sigma [\times 10^3]$	B	m [Kbps]	$\sigma [\times 10^3]$	B
Movie										
Jurassic Park	203	13	15	9.1	157	63	4.0	392	151	3.1
The Silence of the Lambs	363	7	11	18.5	88	53	5.3	219	129	4.5
Star Wars	130	9	13	13.4	112	64	4.0	279	155	3.9
Sports										
Soccer	106	27	26	6.7	326	124	3.9	814	295	2.9
Tennis	121	22	20	8.7	263	98	3.0	657	234	2.8
Race	86	31	21	6.6	369	139	3.6	923	330	3.1
Show										
Talk Show	183	15	17	7.3	174	57	2.7	436	138	2.6
News Show	173	21	26	9.4	248	108	3.8	620	266	3.5
Others										
MTV	134	25	23	9.3	295	138	4.3	738	314	3.9
Video Conference	438	6	12	7.7	72	12	2.0	181	35	1.7

$0, 1, 2, \dots$) be a wide-sense stationary stochastic process with mean m , variance σ^2 , and autocorrelation function $r(k), k \geq 0$. X is said to exhibit the LRD characteristic if, for $0 < D < 1$, $r(k)$ is expressed as

$$r(k) \simeq k^{-D}, \quad \text{as } k \rightarrow \infty, \quad (1)$$

where k is a lag index. However, in video traffic with the short-range dependence (SRD) characteristic, for $0 < p < 1$, $r(k)$ is approximated by

$$r(k) \simeq \rho^k, \quad \text{as } k \rightarrow \infty. \quad (2)$$

If video traffic with the LRD characteristic is approximated by the conventional traffic represented by the SRD characteristic, the correlation is underestimated.

3.2. Hurst Parameter Estimation Methods

The fractal dimension is an important statistical characteristic of a fractal signal with geometrical structure [7, 8]. Stationary stochastic processes with the LRD characteristic

TABLE II
Parameters of the MPEG Bit Stream Encoder

Picture rate	30 (frames/sec)
GOP size	12 frames
Pattern	IBBPBBPBBPBB IBBPBB...
Encoder input	384 × 288 pels
Motion vector search	'Logarithmic'/'Simple'
Color format	YUV (4:1:1, resolution of 8 bits)
Reference frame	'Original'
Quantization values	I = 10, P = 14, B = 18
Slices	1
Vector/range	half pel/10

where α denotes a constant. The power spectrum $P_{2^j}(w)$ of a fractal signal filtered by the high pass filter $\hat{\psi}_{2^j}(w)$ is expressed as

$$P_{2^j}(w) = P(w)|\hat{\psi}(2^{-j}w)|^2, \quad (7)$$

where $\hat{\psi}_{2^j}(w) = \hat{\psi}(2^{-j}w)$ denotes the wavelet function at resolution 2^j . The power spectrum $P_{2^j}^d(w)$ of a discrete signal, sampled by a factor of 2^j , is written as

$$P_{2^j}^d(w) = 2^j \sum_{m=-\infty}^{+\infty} P_{2^j}(w + 2^j 2m\pi). \quad (8)$$

Let $\sigma_{2^j}^2$ be the energy of a high frequency signal $D_{2^j} f$, defined by

$$\sigma_{2^j}^2 = \frac{2^{-j}}{2\pi} \int_{-2^j\pi}^{+2^j\pi} P_{2^j}^d(w) dw. \quad (9)$$

By putting (7) and (8) into (9), we obtain the relationship

$$\sigma_{2^j}^2 = 2^{2H} \sigma_{2^{j+1}}^2. \quad (10)$$

Thus the Hurst parameter is computed by

$$H = \frac{1}{2} \log_2 \frac{\sigma_{2^j}^2}{\sigma_{2^{j+1}}^2}. \quad (11)$$

Note that the ratio $\sigma_{2^j}^2/\sigma_{2^{j+1}}^2$ is a constant.

3.2.3. Line length method. All points are covered by a surface with a blanket of thickness 2ϵ . Then the line length denotes the area occupied by the blanket with thickness 2ϵ [12]. Let $g(x)$ be the function value at point x , u_ϵ denote upper surface, and b_ϵ represent lower surface. Initial values for upper and lower surfaces are given by $u_0(x) = b_0(x) = g(x)$. Then the blanket surfaces are recursively defined by, for $\epsilon = 1, 2, 3, \dots$,

$$u_\epsilon(i) = \max\{u_{\epsilon-1}(i) + t, \max u_{\epsilon-1}(j)\} \quad (12)$$

and

$$b_\epsilon(i) = \min\{b_{\epsilon-1}(i) - t, \min b_{\epsilon-1}(j)\}, \quad (13)$$

where point j is the point with the distance from point i less than or equal to one, $|j - i| \leq 1$, and t denotes the thickness parameter. The current value of the upper (lower) surface is increased (decreased) by the thickness parameter t , and the maximum (minimum) value is selected among the increased (decreased) surface value and surface values of its neighbors. The area a_ϵ of the blanket is obtained in terms of u_ϵ and b_ϵ :

$$a_\epsilon = \sum_i (u_\epsilon(i) - b_\epsilon(i)). \quad (14)$$

The line length $L(\epsilon)$ is computed by

$$L(\epsilon) = \frac{a_\epsilon - a_{\epsilon-1}}{2} \quad (15)$$

and the length of a fractal surface is expressed by

$$L(\epsilon) = F\epsilon^{2-D}, \quad (16)$$

where F is a constant and D represents the fractal dimension. The relationship between the Hurst parameter and fractal dimension is expressed as

$$H = T + 1 - D, \quad (17)$$

where T represents the topological dimension. In the case of one-dimensional video data, T is equal to one.

3.2.4. Fourier filtering method. The Hurst parameter can be computed in the frequency domain [13]. In a finite time interval $0 < t < T$, the process $X(t, T)$ is given by

$$X(t, T) = \begin{cases} X(t), & 0 < t < T \\ 0, & \text{otherwise.} \end{cases} \quad (18)$$

The Fourier transform $F(f, T)$ of $X(t, T)$ is defined by

$$F(f, T) = \int_0^T X(t, T)e^{-j2\pi ft} dt, \quad (19)$$

where $j = \sqrt{-1}$ and the power spectral density $S(f, T)$ of $X(t, T)$ is expressed as

$$S(f, T) = \frac{1}{T} |F(f, T)|^2. \quad (20)$$

The power spectral density $S(f)$ of X is defined by

$$S(f) = \lim_{T \rightarrow \infty} \frac{1}{T} |F(f, T)|^2, \quad (21)$$

where $S(f)$ is a nonnegative and even function. The power spectral density is inversely proportional to f^β ,

$$S(f) \propto \frac{1}{f^\beta}, \quad (22)$$

and the Hurst parameter H is related to β ,

$$H = \frac{\beta - 1}{2}, \quad (23)$$

which indicates that the Hurst parameter is a linear function of β .

3.3. Fractal Modeling

The fractional autoregressive integrated moving average (F-ARIMA) (p, d, q) process is a stationary process showing both LRD and SRD characteristics [14]. For the autoregressive moving average (ARMA) (p, q) process, X_t is expressed as

$$X_t = \phi_1 X_{t-1} + \phi_2 X_{t-2} + \dots + \phi_p X_{t-p} + \varepsilon_t - \theta_1 \varepsilon_{t-1} - \theta_2 \varepsilon_{t-2} - \dots - \theta_q \varepsilon_{t-q}, \quad (24)$$

where ε_t is uncorrelated Gaussian noise and θ_j and ϕ_j are real coefficients. X_{t-m} , $1 \leq m \leq p$, is a correlated normally distributed random variable. A lag operator B is defined by the relationship

$$X_{t-1} = B X_t \quad (25)$$

and the difference operator ∇ is defined by

$$\nabla X_t = (X_t - X_{t-1}) = (1 - B)X_t. \quad (26)$$

For real d , $\nabla^d X_k$ is expressed as

$$\nabla^d X_k = \sum_{i=0}^{\infty} \binom{d}{i} (-1)^i X_{k-1}, \quad -\frac{1}{2} < d < \frac{1}{2}, \quad (27)$$

where $\binom{d}{i} (-1)^i$ is represented by

$$\binom{d}{i} (-1)^i = \frac{\Gamma(-d + i)}{\Gamma(-d)\Gamma(i + 1)} \quad (28)$$

with the gamma function $\Gamma(x)$ defined by $\int_0^{\infty} t^{x-1} e^{-t} dt$. Let $\phi(B)$ and $\theta(B)$ be polynomials of the operator B . The autoregressive coefficient $\phi(B)$ and the moving average coefficient $\theta(B)$ are represented by

$$\phi(B) = (1 - \phi_1 B - \dots - \phi_p B^p) \quad (29)$$

$$\theta(B) = (1 - \theta_1 B - \dots - \theta_q B^q). \quad (30)$$

Then the F-ARIMA (p, d, q) process is expressed as

$$\phi(B)\nabla^d X_t = \theta(B)\varepsilon_t. \quad (31)$$

To generate the F-ARIMA process, X_t satisfying (31) must be generated. As the F-ARIMA process, a simple F-ARIMA(1, d , 0) process is commonly used, in which the equation

$$(1 - \phi_1 B)\nabla^d X_t = \varepsilon_t \quad (32)$$

is used. Equation (32) is expressed as

$$(1 - \phi_1 B) \left(\sum_{i=1}^{\infty} \binom{d}{i} (-1)^i X_{k-i} + X_k \right) = \varepsilon_t \quad (33)$$

and X_k is written as

$$\begin{aligned} X_k &= (\phi_1 B - 1) \left(\sum_{i=1}^{\infty} \binom{d}{i} (-1)^i X_{k-i} \right) + \phi_1 X_{k-1} + \varepsilon_t \\ &= (\phi_1 B - 1) \left(\sum_{i=1}^{\infty} \frac{\Gamma(-d+i)}{\Gamma(-d)\Gamma(i+1)} X_{k-i} \right) + \phi_1 X_{k-1} + \varepsilon_t. \end{aligned} \quad (34)$$

For $0 < d < 1/2$, the F-ARIMA process is stationary and shows the LRD characteristic. The SRD structure is controlled by changing $\phi(B)$ and $\theta(B)$, whereas the LRD structure is controlled by changing d .

4. BANDWIDTH ALLOCATION

ATM networks must process all services possible in future communication networks. N-ISDN services such as telephone, facsimile, remote sensing, teletext, and e-mail, and B-ISDN services such as video telephone, video conference, color facsimile, CATV, and HDTV are required.

The most important feature of services in ATM networks is that the distribution ranges of bandwidth are very wide. The basic signal of N-ISDN is distributed around 64 Kbps of audio signals, whereas the bandwidth of B-ISDN is extended to hundreds of Mbps. Thus, the efficient bandwidth allocation method is required in ATM networks [15, 16].

Effective bandwidth allocation for video traffic is difficult. Some reasons are as follows: real VBR video traffic exhibits highly bursty and nonstationary properties which complicate the queueing analysis, and the effective bandwidth must avoid buffer blocking and excessive delay by the worst-case video input signal [17].

4.1. Bandwidth Allocation Methods

4.1.1. Deterministic bandwidth allocation method. Allocating the maximum bit rate, the deterministic bandwidth allocation method does not offer necessary adaptability in processing the different kinds of traffic requiring variable bit rates and various bandwidths. It also does not use the statistical characteristics of input traffic, resulting in bandwidth waste. Therefore, it is not suitable for ATM networks. However, it has been widely used in the exchange network of telephone circuits and is suitable for STM.

4.1.2. Statistical bandwidth allocation method. To effectively utilize network resources and the statistical variation of traffic, the statistical bandwidth allocation method considers the types of services. That is, the bandwidth to be allocated is determined by considering the average bit rate of traffic, the maximum bit rate, and the burst characteristics. This method is usually suitable for ATM traffic showing VBR characteristics.

4.2. System Model

Figure 4 shows the system model consisting of a video server, an ATM network, a playback buffer, and an MPEG decoder [18]. Let the size of the i th frame be equal to a_i bits, $i = 1, 2, \dots, n$, where n denotes the number of frames of encoded MPEG bit streams. The bit stream with frame period τ is decoded at a rate of $1/\tau$ frames per second and T_i

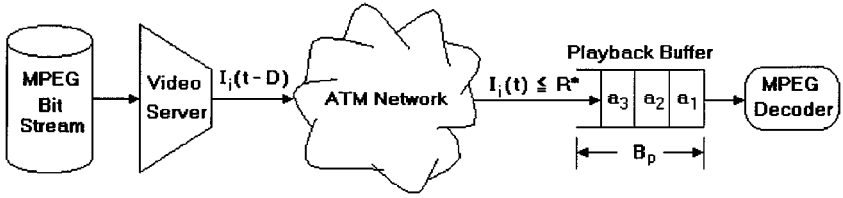


FIG. 4. System model for video server applications.

denotes the time interval for each frame i . The minimum reservation rate, R^* (bps), is the minimum rate at which the bandwidth must be reserved in the ATM network to ensure that the playback buffer does not overflow and is defined by

$$R^* = \max \frac{a_i + \dots + a_j - B_p}{T_i + \dots + T_j} \quad (35)$$

for $1 \leq i \leq j \leq n$, where $a_i + \dots + a_j$ denotes the sum of the frame sizes from the i th to the j th frame, $T_i + \dots + T_j$ represents the sum of the frame periods from the i th to the j th frame, and B_p signifies the size of the playback buffer.

The video server calls the bandwidth R^* to ATM networks. The admission for the call of resources is determined by a call admission control (CAC) algorithm.

The buffer input rate I_i is defined by the rate at which data are received by the playback buffer during the i th frame interval. This is equivalent to the rate at which the server sends out data during the time interval τ . It is the highest rate that does not cause the playback buffer to overflow, not exceeding the minimum reservation rate R^* ($I_i \leq R^*$).

5. EXPERIMENTAL RESULTS AND DISCUSSIONS

The LRD characteristic in VBR MPEG video traffic is investigated, and the performance of the four Hurst parameter estimation methods used in LRD analysis is compared. Statistical characteristics of video data used in the experiments are shown in Tables I and II. The compression rate is inversely proportional to the mean bit rate for the same frame size. It is possible to estimate the amount of change of the traffic by the compression rate. The standard deviation of the bit rate is used to analyze the statistical characteristic of a signal. In Fig. 2, because the different types of traffic do not follow Gaussian distribution, the standard deviation of the bit rate is not related to the compression rate, mean bit rate, and burstiness.

In the F-ARIMA(1, d , 0) process, the LRD characteristic is controlled by changing d , whereas the SRD characteristic is controlled by changing ϕ_1 . Figure 5 shows the Hurst parameter of the F-ARIMA(1, d , 0) process as a function of d for various ϕ_1 values. In our simulations, the interval of d is set to 0.01, and the values of ϕ_1 are set to 0.0, 0.2, 0.4, and 0.6. As d becomes large, the Hurst parameter increases. The detected Hurst parameter slightly varies with different values of ϕ_1 . If d is small (large), data show the SRD (LRD) characteristic. The corresponding equations of Fig. 5 are as follows: (a) $H = 0.93d + 0.46$, (b) $H = 0.82d + 0.47$, (c) $H = 0.79d + 0.48$, and (d) $H = 0.76d + 0.49$. As ϕ_1 increases, the slope decreases ($0.93 \rightarrow 0.82 \rightarrow 0.79 \rightarrow 0.76$). As d increases (near 0.5), the slope becomes relatively flat. From Fig. 5, it is noted that as ϕ_1 and d become large, the relationship $H = d + 0.5$, between the Hurst parameter and d , is no longer true.

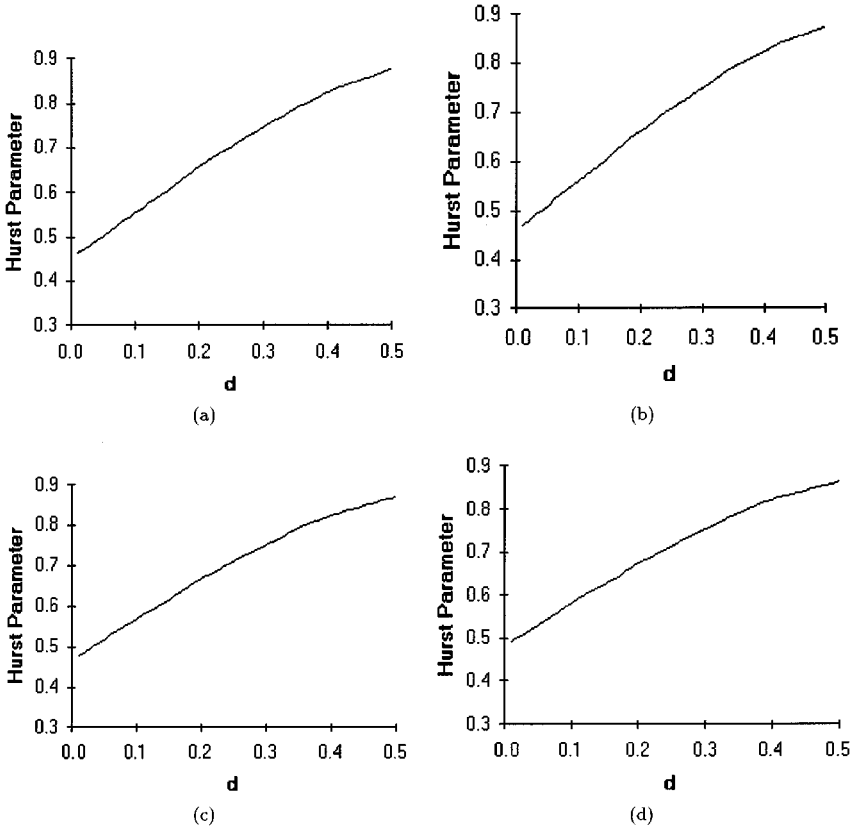


FIG. 5. Comparison of the Hurst parameter of the F-ARIMA(1, d , 0) process as a function of d for various ϕ_1 values: (a) $\phi_1 = 0.0$; (b) $\phi_1 = 0.2$; (c) $\phi_1 = 0.4$; (d) $\phi_1 = 0.6$.

Figure 6 shows a comparison of Hurst parameters estimated by four methods as a function of d for the composite sequence. It is shown that the detected Hurst parameter depends on ϕ_1 . The results for four methods are almost the same. As d becomes large, the detected Hurst parameter also increases, with a similar slope for each method.

Table IIIa shows the Hurst parameter estimated by R/S analysis as a function of nonoverlapping block size. With the size of the sample X_k equal to N , the whole sequence is divided into K nonoverlapping blocks. Then the previous samples are rescaled, and $R(t_i, d)/S(t_i, d)$

TABLE III
Hurst Parameters Estimated by R/S Analysis (Jurassic Park and Soccer Sequences)

(a) A function of nonoverlapping block size				
Block size	1	10	50	100
Jurassic Park	0.88	0.88	0.88	0.88
Soccer	0.91	0.91	0.91	0.91
(b) Parameters calculated framewise				
Frame	I	P	B	Total
Jurassic Park	0.88	0.88	0.89	0.88
Soccer	0.90	0.91	0.90	0.91

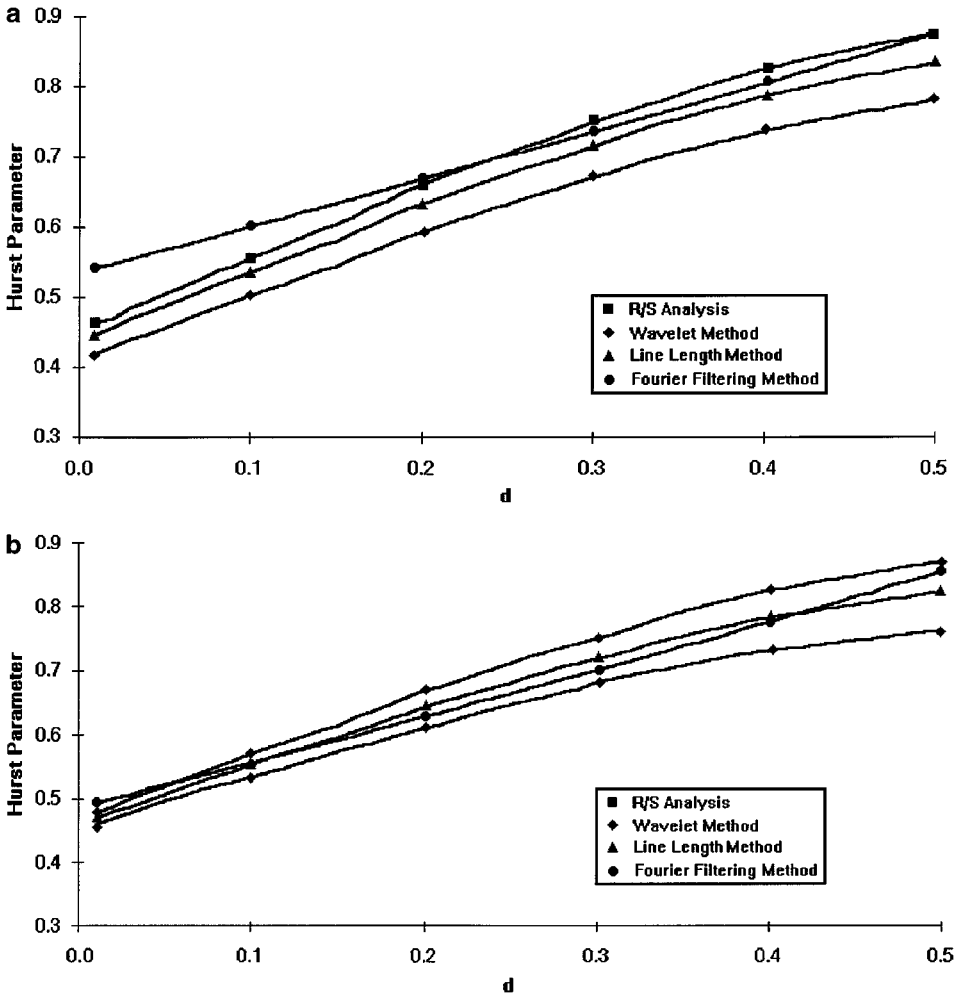


FIG. 6. Comparison of Hurst parameters estimated by four methods for the composite sequence: (a) $\phi_1 = 0.0$; (b) $\phi_1 = 0.4$.

is computed for each sequence, with the new starting point t_i : $t_1 = 1$, $t_2 = (N/K) + 1$, $t_3 = (2N/K) + 1$, \dots , where $(t_i - 1) + d \leq N$, and the nonoverlapping block size is equal to N/K . Experimental results show that the Hurst parameter is independent of the block size; however, small block size requires a high computational load for Hurst parameter estimation. So selection of the proper block size is required and 10 is generally used. If the block size is too large, the H value can be estimated incorrectly. But the data size used in experiments is extremely large; the Hurst parameter can be estimated properly with the block size of 100. Table IIIb shows the Hurst parameters calculated framewise. If the Hurst parameter is estimated in the I frame, with the block size equal to 1/12 of the block size applied to the entire frame, it is similar to that estimated over the entire frame.

In Fig. 7, the Hurst parameters detected by four methods are compared. R/S analysis is used to estimate the Hurst parameter of VBR MPEG video traffic, whereas wavelet, line length, and Fourier filtering methods are employed for estimation of the fractal dimension. The range of the Hurst parameter, $0.5 < H < 1$, is used experimentally for all data, which means that all data show the LRD characteristic. If the Hurst parameter of an input data

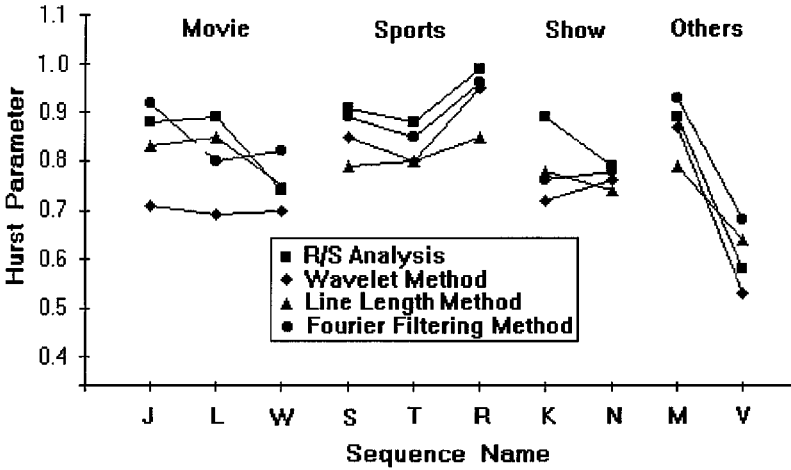


FIG. 7. Comparison of Hurst parameters estimated by four methods for various sequences.

signal is known, we can classify the VBR video scene depending on its activity. For example, the data with low activity have an H value between 0.5 and ~ 0.75 . The data with medium activity have an H value between ~ 0.75 and ~ 0.90 . The data with high activity have an H value between about 0.90 and 1.00. Hurst parameters estimated by R/S analysis differ from those estimated by other methods. It is important to correctly estimate Hurst parameters to effectively examine the LRD characteristic of the traffic. Hurst parameter values of real data are unknown, so the performance of each method cannot be fairly compared. In experiments, sports sequences show large motions whereas the Video Conference sequence shows small motions. The Hurst parameter of the former is also large, whereas that of the latter is small for all methods. Note that the Hurst parameter is related to the amount of motions involved in the sequence.

R/S analysis requires relatively small computational load in which it is important to select the nonoverlapping block size for computational efficiency. Experimentally, the nonoverlapping block size is set to 10 for trade-off between the computational efficiency and accuracy, in which the Hurst parameter is almost the same for different nonoverlapping block sizes. In the wavelet method, the Hurst parameter value depends on the number of decomposition layers employed. Experimentally, two-layer decomposition gives the results similar to those by other methods. A large number of decomposition layers requires high computational complexity. The line length method is the simplest of the four methods in terms of the computational efficiency, although it is difficult to select a thickness parameter t in (12) and (13). Experimentally, we set $t = 100$ for MPEG video traffic with the mean frame rate greater than 1000 bits. Note that the thickness has to be set differently depending on the traffic characteristic of the video sequence. The Fourier filtering method requires a relatively high computational load; thus, it is not suitable for real-time applications.

Thus far, the Hurst parameter has been estimated over the entire frame of the sequence. However, the areas containing large and small motions coexist even in a single sequence. So the local estimation of the Hurst parameter is required, for which a proper frame size is to be selected. Figure 8 shows the Hurst parameter as a function of the frame size, from which the proper frame size is selected for local Hurst parameter estimation of VBR MPEG

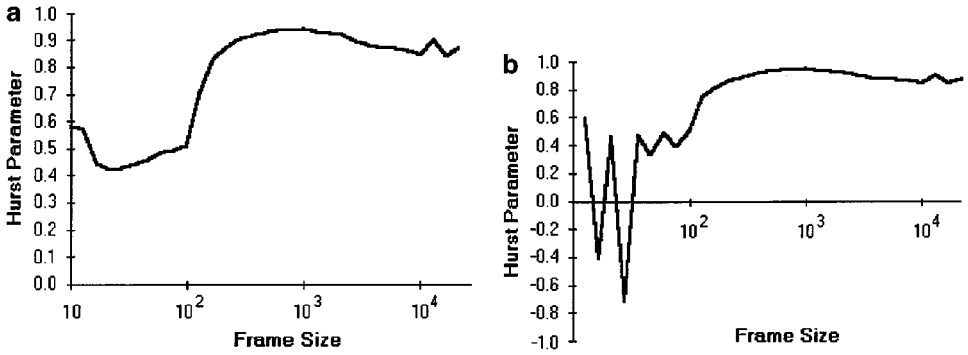


FIG. 8. Local Hurst parameters as a function of the frame size: (a) nonoverlapping block size = 10; (b) nonoverlapping block size = 1.

video sequence. Figure 8a shows the Hurst parameter as a function of the frame size when the nonoverlapping block size is set to 10. The recontrolled frame number is less than 10 when the frame number is less than 100. The Hurst parameter fluctuates, especially when the sample size is very small. The Hurst parameter must be positive, and for the traffic with the LRD characteristic, it should be larger than 0.5.

Figure 8b shows the Hurst parameter as a function of the frame size when the nonoverlapping block size is equal to 1. The Hurst parameter has a value smaller than 0.5 when the frame size is less than 100. However, when the frame size is larger than 500, the Hurst parameter can be estimated properly and a constant Hurst parameter is obtained regardless of the block size. The estimation of the Hurst parameter is severely biased unless the short-range correlations are suppressed through aggregation or filtering. In (5), for very small n , H may have a negative value. For meaningful estimation of the local Hurst parameter, a frame size larger than 500 frames is required.

Figure 9 shows the mean, variance, peak/mean, variance/mean², and Hurst parameter estimated for two cases with 40 subsequences. The Jurassic Park sequence with 40,000 frames is segmented into 40 nonoverlapping subsequences. Figures 9a, 9c, 9e, 9g, and 9i show the results for the nonaccumulated sequences, whereas Figs. 9b, 9d, 9f, 9h, and 9j are the results for the accumulated sequences, where the accumulated sequence denotes the sequence obtained by concatenating a number of nonoverlapping subsequences. The distribution of various statistical measures is shown in Fig. 9. The estimated Hurst parameter value shows fluctuation around 0.87 in Fig. 9i, and the local Hurst parameter estimated from the nonaccumulated sequence is different from that estimated over the entire sequence. Figure 9 shows that the statistical characteristics of the accumulated sequence have similar values if the frame size is larger than some threshold value. A sequence with a similar statistical measure consists of subsequences with different statistical characteristics. In experiments, the Hurst parameter of the Jurassic Park sequence estimated with 15,000 frames is similar to that estimated with the entire sequence of 40,000 frames.

The Hurst parameter represents the fractal characteristic of VBR MPEG video traffic; i.e., it describes the long-range dependence characteristic of video traffic. It is not related to the mean bit rate of video traffic, but it is instead related to the standard deviation and burstiness in the sense that it represents the amount of traffic variation of the video sequence. Experimental results show that it is not directly proportional to the standard deviation and burstiness of the video sequence.

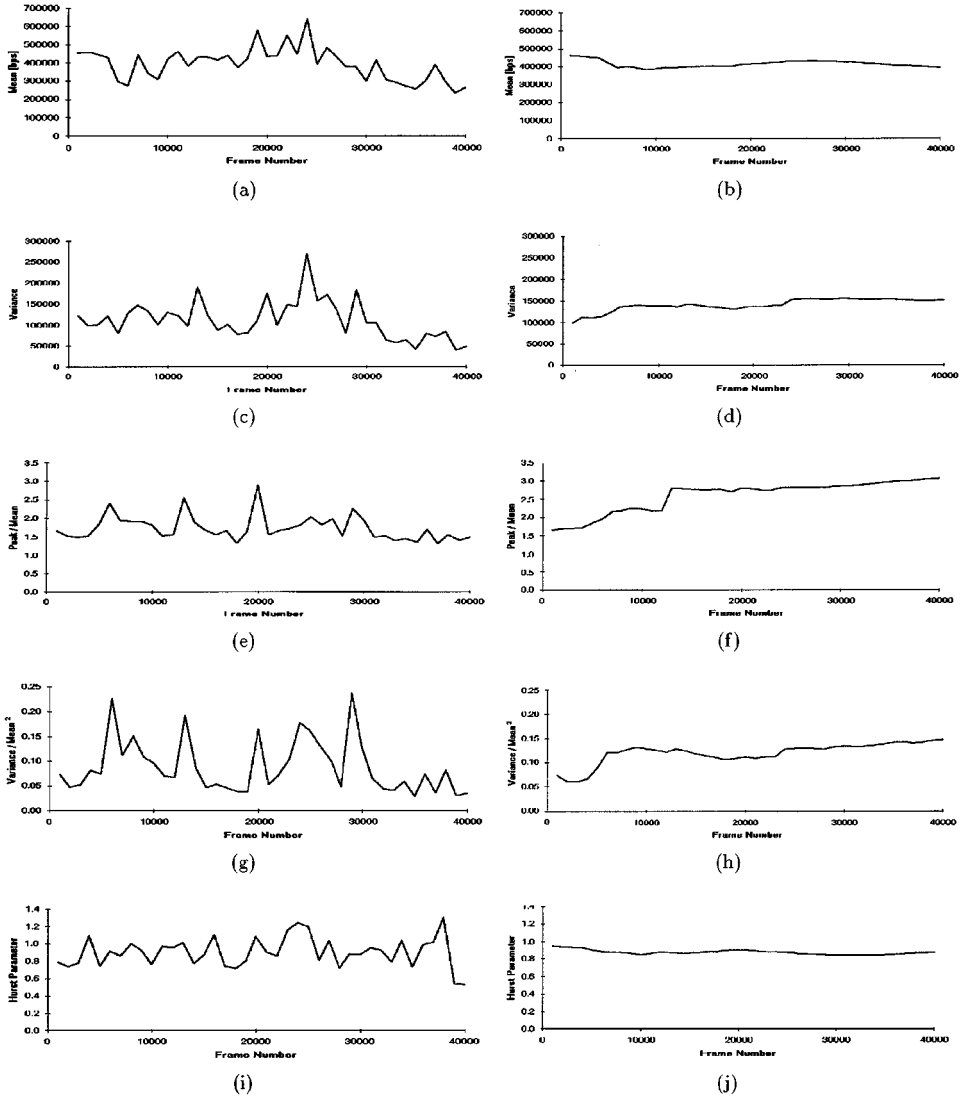


FIG. 9. Statistical characteristics of the Jurassic Park sequence (40 subsequences of 1000 frames each): (a) mean (nonaccumulated); (b) mean (accumulated); (c) variance (nonaccumulated); (d) variance (accumulated); (e) peak/mean (nonaccumulated); (f) peak/mean (accumulated); (g) variance/mean² (nonaccumulated); (h) variance/mean² (accumulated); (i) Hurst parameter (nonaccumulated); (j) Hurst parameter (accumulated).

Figure 10 shows comparison of the minimum reservation rate as a function of the buffer size for various sequences, where the minimum reservation rate represents the minimum bandwidth without buffer overflow. The larger the buffer size, the smaller the minimum bandwidth reservation rate. The Sports sequences and the TV sequences with large Hurst parameters give large minimum reservation rates whereas the Video Conference sequence with small Hurst parameters yields a small minimum reservation rate. The sequence with a large Hurst parameter shows large motions and data size, requiring large bandwidth.

If the buffer size increases to infinity, the minimum reservation rate is equal to the average bit rate listed in Table I. Practically, a very large buffer size cannot be allocated as the trade-off between the bandwidth utilization and the cell loss.

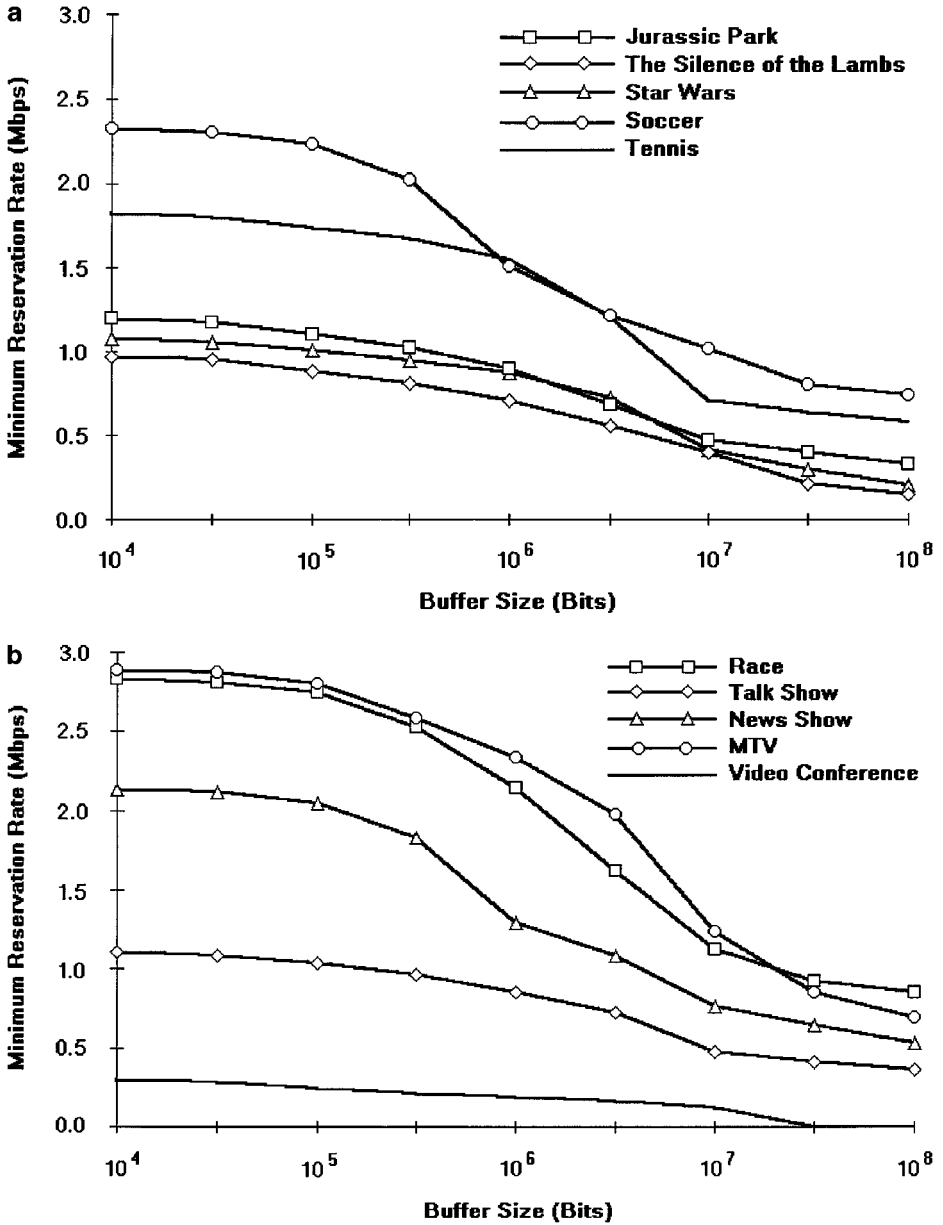


FIG. 10. Comparison of the minimum reservation rate as a function of the buffer size for various sequences.

The mean bit rate, minimum reservation rate, and Hurst parameter for several test sequences are listed in Table IV, in which the Hurst parameter specifies the average of four Hurst parameter values obtained by four estimation methods. It is noted that the minimum reservation rate is roughly proportional to the mean bit rate times the Hurst parameter. But this relationship is not always true because the estimated Hurst parameters are different for various estimation methods, as shown in Fig. 7. The Hurst parameter is not the only factor for bandwidth allocation because it is related to the burst characteristic of the traffic. Therefore, other traffic information is needed for efficient bandwidth allocation.

TABLE IV
Hurst Parameter and Minimum Reservation Rate of Each Video Sequence

Sequence	R	m (Kbps)	Original source size (Mbps)	Hurst parameter (H)	$m \times H$	MRR (Mbps) BS = 10^5	Normalized MRR (Kbps) BS = 10^5
Jurassic Park	203	392	79.60	0.83	325	1.1	281
The Silence of the Lambs	363	213	77.28	0.81	177	0.9	411
Star Wars	130	279	36.24	0.75	209	1.0	358
Soccer	106	814	86.32	0.86	700	2.2	270
Tennis	121	657	79.52	0.79	529	1.8	274
Race	88	923	79.36	0.94	867	2.7	293
Talk Show	183	436	79.76	0.79	344	1.0	229
News Show	173	620	107.28	0.77	477	2.1	339
MTV	134	738	98.88	0.87	568	2.8	379
Video Conference	938	181	79.28	0.61	110	0.3	166

The bandwidth in ATM networks cannot be allocated by a single parameter of input traffic. Thus, the minimum number of parameters is used, for which the Hurst parameter and the average bit rate can be used for bandwidth allocation. The average bit rate determines the distribution range, whereas the Hurst parameter shows the activity of the input traffic. For the same mean traffic value, the larger the Hurst parameter, the larger the bandwidth allocation. So the Hurst parameter is proportional to the minimum reservation rate. But we must consider parameters such as delay when considering the VBR video traffic with very complex motions.

Table IV shows the compression rate, mean bit rate, original source size (compression rate \times mean bit rate), and normalized minimum reservation rate (MRR) with buffer size (BS) equal to 10^5 for several examples VBR MPEG video traffic. The normalized minimum reservation rate is the value when the mean bit rate is set to 100 Kbps. The original source sizes are almost the same except for the Star Wars, News Show, and MTV sequences. The Hurst parameter is not explicitly related to the mean bit rate, but it depends on the activity of video traffic. The larger the activity of video traffic, the larger the Hurst parameter. If a video stream has a larger activity, it requires a larger minimum reservation rate for the same mean bit rate. For the same activity, the minimum reservation rate depends on the mean bit rate. Thus, the minimum reservation rate is roughly proportional to the mean bit rate times the Hurst parameter. So the larger the Hurst parameter and mean bit rate are, the larger the bandwidth. Note that the minimum reservation rate is approximately proportional to the mean bit rate times the Hurst parameter. Figure 11 shows the relationship between the minimum reservation rate and the mean bit rate times the Hurst parameter for ten test sequences. There are small fluctuations, but the minimum reservation rate is approximately proportional to the mean bit rate times the Hurst parameter.

Table V shows the relationship between the minimum reservation rate and the mean bit rate times the Hurst parameter for four different Hurst parameter estimation methods (R/S; R/S analysis; WM, wavelet method; LL, line length method; and FF, Fourier filtering method). The line length method has the mean bit rate times the Hurst parameter value smaller than that of other methods, with the other methods except for the line length method showing similar values. Note that the line length method requires less computation time and complexity. Figure 12 shows the relationship between the minimum reservation rate and the

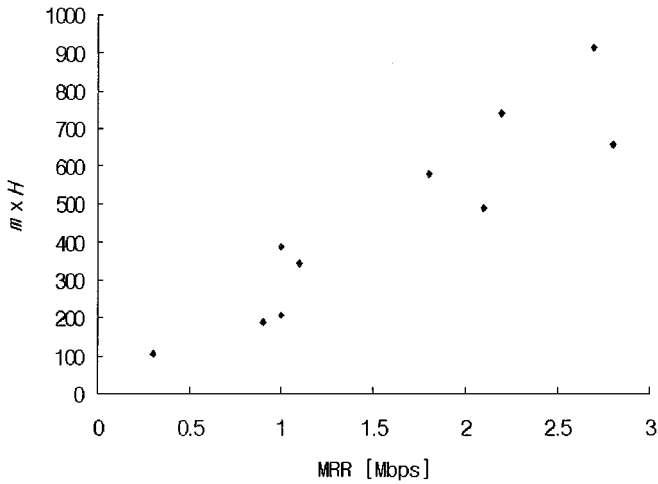


FIG. 11. Relationship between the minimum reservation rate and the mean bit rate times the Hurst parameter for ten test sequences.

mean bit rate times the Hurst parameter for four Hurst parameter estimation methods. The shapes of graphs for each method are somewhat different, but for all cases the minimum reservation rate is approximately proportional to the mean bit rate times the Hurst parameter.

Figure 13 shows the relationship between the minimum reservation rate and the mean bit rate times the Hurst parameter for several buffer sizes (10^4 , 10^5 , 10^6 , and 10^7). The minimum reservation rate is approximately proportional to the mean bit rate times the Hurst parameter for different buffer sizes. The most important factor of estimation conditions is the buffer size. The determination of buffer size is related to the mean bit rate. If the buffer size is too large, bandwidth allocation control is not important, which is difficult in real networks. Less bandwidth allocation is needed to guarantee no buffer overflow.

It was presented [19] that the stochastic process $V(\alpha t)$ has a service rate given by

$$m + \alpha^{(1-H)}(C - m),$$

where m represents the mean input rate, α denotes an arbitrary number, C is the service rate of $V(t)$, and H signifies the Hurst parameter. This expression shows that the service rate

TABLE V

Comparison of the Relationship between the Minimum Reservation Rate and the Mean Bit Rate Times the Hurst Parameter for Each Hurst Parameter Estimation Method

Sequence	R/S		WM		LL		FF	
	H	$m \times H$	H	$m \times H$	H	$m \times H$	H	$m \times H$
Jurassic Park	0.88	345	0.71	278	0.83	325	0.92	361
The Silence of the Lambs	0.89	190	0.70	149	0.84	179	0.80	170
Star Wars	0.74	206	0.70	195	0.74	206	0.82	229
Soccer	0.91	741	0.85	692	0.79	643	0.89	724
Tennis	0.88	578	0.80	526	0.80	526	0.86	565
Race	0.99	914	0.85	785	0.84	775	0.96	886
Talk Show	0.89	388	0.72	314	0.78	340	0.77	336
News Show	0.79	490	0.76	471	0.78	484	0.78	484
MTV	0.89	657	0.87	642	0.79	583	0.93	686
Video Conference	0.58	105	0.53	100	0.64	116	0.68	123

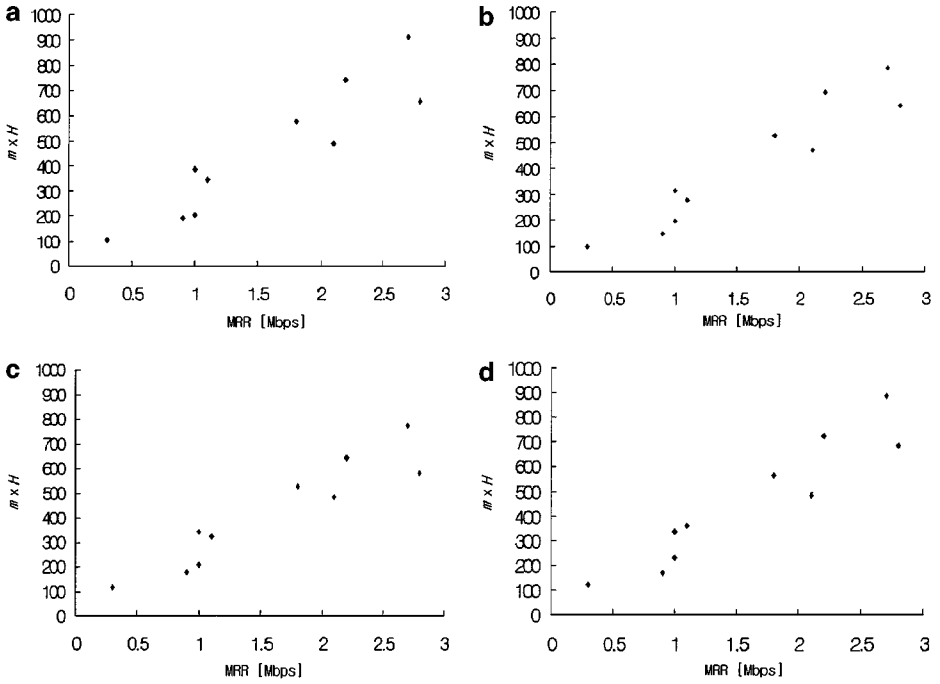


FIG. 12. Relationship between the minimum reservation rate and the mean bit rate times the Hurst parameter for four Hurst parameter estimation methods: (a) R/S analysis; (b) wavelet method; (c) line length method; (d) Fourier filtering method.

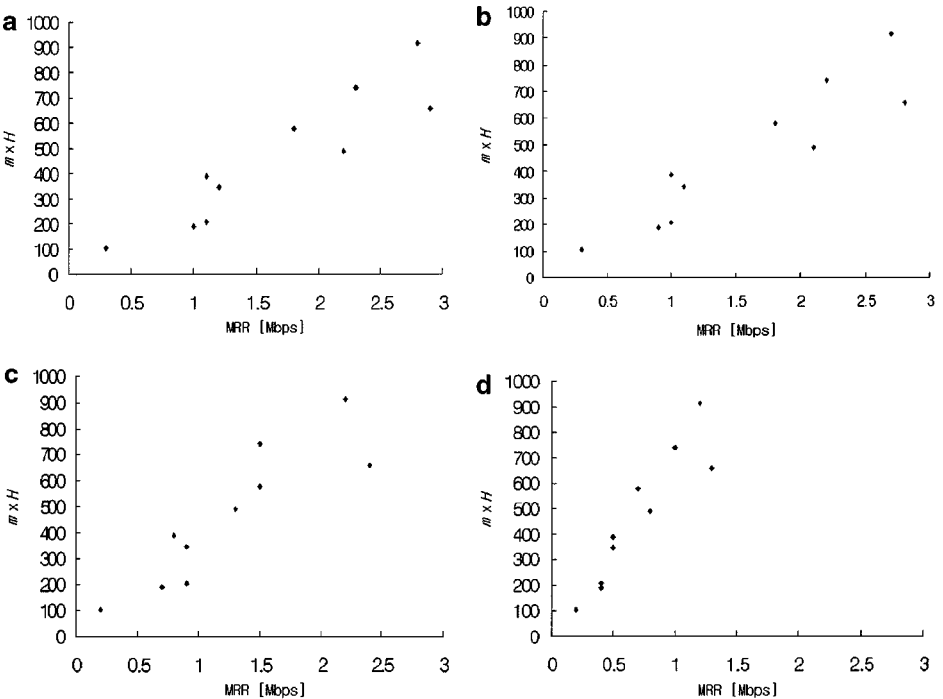


FIG. 13. Relationship between the minimum reservation rate and the mean bit rate times the Hurst parameter for different buffer sizes: (a) buffer size = 10^4 ; (b) buffer size = 10^5 ; (c) buffer size = 10^6 ; (d) buffer size = 10^7 .

depends on the mean bit rate and the Hurst parameter; however, it is not directly proportional to them. In this equation, H characterizes the quality of the traffic, whereas m characterizes its quantity. The bandwidth allocation is related to both terms. The second term can have a bigger or smaller value than the first term depending on α . Both quality and quantity are important in bandwidth allocation. To apply this equation to actual sequences, α must be properly determined.

The Hurst parameter shows the characteristic of traffic: the characteristic of long-time traffic is represented by the Hurst parameter. In allocating the bandwidth, it is not desirable to use a large number of variables because the bandwidth allocation is to be processed in real time. For direct calculation of the required minimum bandwidth of a video stream, we can use (35). But it is difficult to select appropriate values of i and j , noting that the minimum reservation varies for different i and j . In such cases, the estimated minimum reservation rate is not suitable for band allocation control of the video bit stream.

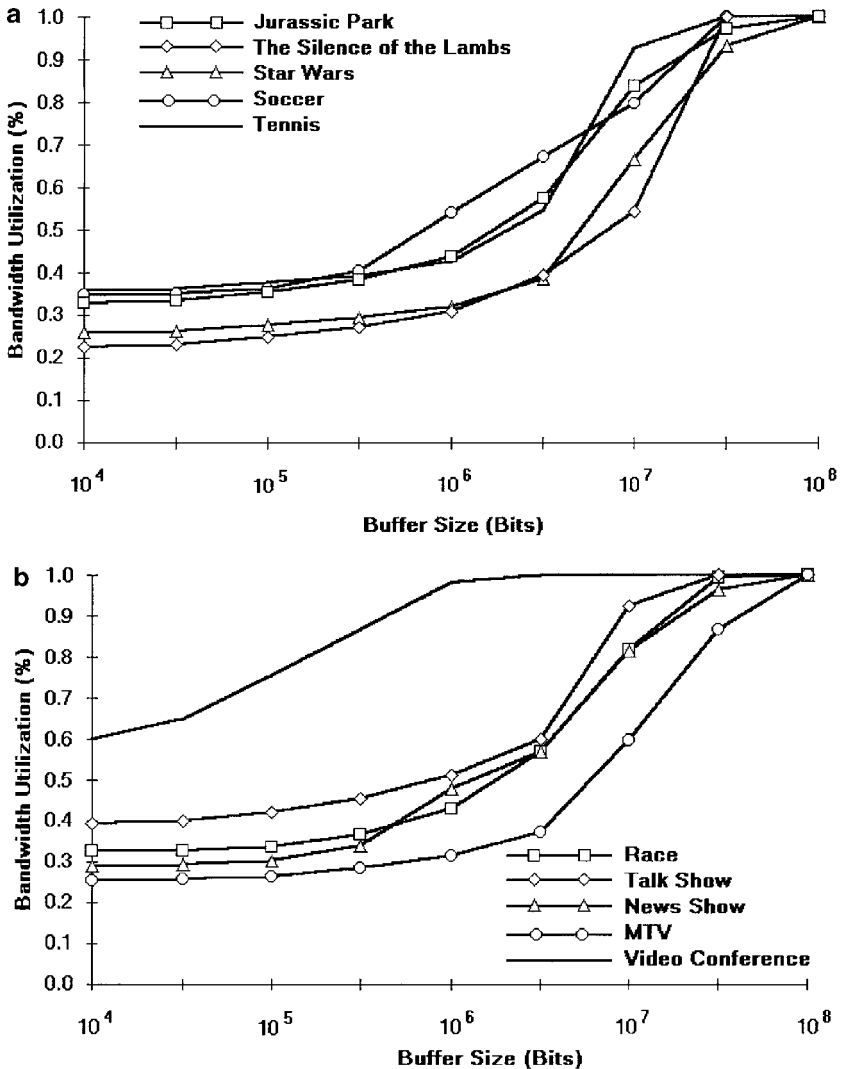


FIG. 14. Comparison of the bandwidth utilization as a function of the buffer size for various sequences.

Figure 14 shows comparison of the bandwidth utilization as a function of the size change for various sequences, where the bandwidth utilization is defined by the ratio of the mean bit rate to the minimum reservation rate. Note that the mean bit rate is shown in Table I and the bandwidth utilization is not definitely related to the minimum reservation rate. In experiments, the bandwidth utilization of the Video Conference sequence with small motions is the largest. If traffic is not bursty, the bandwidth can be utilized better by small bandwidth allocation. However, in ATM networks, most traffic shows different characteristics, so the adaptive bandwidth allocation method is desirable.

6. CONCLUSION

The Hurst parameter is used to measure the activity of video traffic showing the LRD characteristic. Three different methods for Hurst parameter estimation of VBR MPEG video traffic are presented and their performance of LRD analysis is compared for various video traffic bit streams. We can classify the activity of video data based on the Hurst parameter value; for example, the data with a large Hurst parameter contain large motions. In the F-ARIMA(1, d , 0) process, the parameter value d is related to the LRD characteristic in the sense that the parameter d is proportional to the Hurst parameter. Further research will focus on applications of Hurst parameter estimation to traffic control of real LRD MPEG video traffic in ATM networks.

REFERENCES

1. S. H. Hong, R.-H. Park, and C. B. Lee, Two-layer video coding and cell-loss concealment using pyramid structures, *J. Electr. Imag.* **7**, 1998, 548–557.
2. C. B. Lee, S. H. Hong, and R.-H. Park, Hurst parameter estimation of VBR MPEG video traffic with long-range dependence in ATM networks, in *Proceedings, Int. Conf. on Telecommunications, ICT '98, Porto Carras, Greece, 1998*, pp. 430–434.
3. B. Maglaris, D. Anastassiou, P. Sen, G. Karlsson, and J. Robbins, Performance models of statistical multiplexing in packet video communications, *IEEE Trans. Commun.* **36**, 1988, 834–843.
4. D. Reiningger, B. Melamed, and D. Raychaudhuri, Variable bit rate MPEG video: Characteristics, modeling and multiplexing, in *Proceedings, 14th Int. Teletraffic Cong. ITC-14, Antibes Juan-les-Pins, France, 1994*, pp. 295–306.
5. M. Krunz, R. Sass, and H. Hughes, Statistical characteristics and multiplexing of MPEG streams, in *Proceedings, IEEE INFOCOM '95, Boston, MA, 1995*, pp. 455–462.
6. O. Rose, *Statistical Properties of MPEG Video Traffic and Their Impact on Traffic Modeling in ATM Systems*, University of Würzburg Institute of Computer Science Research Report Series, Report 101, Feb. 1995. [The VBR MPEG video traces used in this research were obtained via anonymous ftp from ftp-info3.informatik.uni-wuerzburg.de in the /pub/MPEG directory.]
7. P. Maragos and F.-K. Sun, Measuring the fractal dimension of signals: Morphological covers and iterative optimization, *IEEE Trans. Signal Process.* **41**, 1993, 108–121.
8. I. Norros, On the use of fractional Brownian motion in the theory of connectionless networks, *IEEE J. Select. Areas Commun.* **13**, 1995, 953–962.
9. J. Beran, R. Sherman, M. S. Taqqu, and W. Willinger, Long-range dependence in variable-bit-rate video traffic, *IEEE Trans. Commun.* **43**, 1995, 1566–1579.
10. W. E. Leland, W. Willinger, M. S. Taqqu, and D. V. Wilson, Statistical analysis and stochastic modeling of self-similar data traffic, in *Proceedings, 14th Int. Teletraffic Cong. ITC-14, Antibes Juan-les-Pins, France, 1994*, pp. 319–328.
11. S. G. Mallat, A theory for multiresolution signal decomposition: The wavelet representation, *IEEE Trans. Pattern Anal. Mach. Intell.* **11**, 1989, 674–693.
12. S. Peleg, J. Naor, R. Hartley, and D. Avnir, Multiple resolution texture analysis and classification, *IEEE Trans. Pattern Anal. Mach. Intell.* **6**, 1984, 518–523.

13. P. Kube and A. Pentland, On the imaging of fractal surfaces, *IEEE Trans. Pattern Anal. Mach. Intell.* **10**, 1988, 704–707.
14. A. Adas and A. Mukherjee, On resource management and QOS guarantees for long range dependent traffic, in *Proceedings, IEEE INFOCOM '95, Boston, MA, 1995*, pp. 779–787.
15. P. Pancha and M. E. Zarki, Bandwidth-allocation schemes for variable-bit-rate MPEG sources in ATM networks, *IEEE Trans. Circuits Syst. Video Technol.* **3**, 1993, 190–198.
16. T.-S. Yum, M.-S. Chen, and Y.-W. Leung, Video bandwidth allocation for multimedia teleconferences, *IEEE Trans. Commun.* **43**, 1995, 457–465.
17. M. W. Garrett and W. Willinger, Analysis, modeling and generation of self-similar VBR video traffic, in *Proceedings, ACM SIGCOMM'94, London, England, 1994*, pp. 269–280.
18. J. Lauderdale and D. H. K. Tsang, A new techniques for transmission of pre-encoded MPEG VBR video using CBR service, in *Proceedings, 1996 IEEE Int. Conf. Commun., Dallas, Texas, 1996*, pp. 1416–1420.
19. I. Norros, A storage model with self-similar input, *Queueing Systems* **6**, 1994, 387–396.